Chemical Physics Letters 660 (2016) 87–92

Contents lists available at ScienceDirect

Chemical Physics Letters

journal homepage: www.elsevier.com/locate/cplett

Research paper

Modeling the atomic-scale structure, stability, and morphological transformations in the tetragonal phase of $LaVO_4$

Amanda F. Gouveia [a], Mateus M. Ferrer [b], Júlio R. Sambrano [b], Juan Andrés [c,*], Elson Longo [a]

[a] CDMF, Universidade Federal de São Carlos (UFSCar), P.O. Box 676, São Carlos 13565-905, Brazil
[b] Modeling and Molecular Simulations Group, São Paulo State University (UNESP), P.O. Box 473, Bauru 17033-360, Brazil
[c] Department of Analytical and Physical Chemistry, University Jaume I (UJI), Castelló 12071, Spain

ARTICLE INFO

Article history:
Received 21 June 2016
In final form 5 August 2016
Available online 6 August 2016

Keywords:
Surface energy
Wulff construction
Morphology
t-$LaVO_4$

ABSTRACT

In this communication, a systematic study of the surface structure, including energy management during morphological transformations of tetragonal phase of $LaVO_4$, has been carried out. For this study, we combined experimental findings and first-principles calculations to develop a Wulff construction model. Our findings can help further understand the synthetic control of crystal shape via tuning of surface chemistry.

1. Introduction

The phrase "structure dictates function" is an established dictum from the field of biology that is now recognized in materials science [1]. In particular, the interplay between the surface structure and morphology of materials and nanomaterials plays a key role in improving the materials' properties and performance, especially for applications in chemistry and chemical engineering fields [2]. There is considerable interest in the effects of the shapes and facets of crystalline materials; it is well known that the atomic configuration of the exposed crystal plane plays an important role in these materials' performance. This is due mainly to the arrangement of the surface atoms and the number of dangling bonds on different crystal planes [3–5].

Anisotropy is a basic property of single crystals, which show different physical and chemical properties on various facets in directions. Usually, these properties can be correlated with the surface energy associated with each facet and can be finely tuned by tailoring the facets to have a specific surface atomic arrangement and coordination, i.e. by tailoring the fraction of surface atoms with unsaturated coordination shells and the number of undercoordinated surface atoms. Measuring the geometries and energies of these surface facets is extremely challenging [6]. Surface energy considerations are crucial in understanding and predicting the morphologies of noble metal nanocrystals. Surface energy is defined as the excess free energy per unit area for a particular crystallographic face. It largely determines the faceting and crystal growth observed with particles at both the nanoscale and mesoscale. Therefore, optimizing the surface-driven attributes of these materials requires a detailed understanding of the structure and chemical composition of their surfaces. With this understanding, one can tailor the surface atomic structure and control which facets of a given material are exposed. Consequently, substantial effort has been devoted to understanding and predicting the structure and stability of complex materials, utilizing state-of-the-art experimental techniques and advanced theoretical approaches [7,8].

Using experimentation to identify the atomistic details involved in a typical crystal growth process is not easy. Computational simulations via density functional theory (DFT) are real alternatives that can provide fresh insight at the atomic scale and thereby specify the important individual atomistic processes taking place during crystal growth. These processes control the final morphology, surface structure, and stability of the end-product materials [9–29]. In addition, there are good reviews on theoretical methods for surface chemistry [30] and the modeling of nanoparticles [31].

By means of experimental and theoretical calculation methods, Li et al. [24] investigated the mechanisms of morphology of tetragonal lanthanum orthovanadate (*t*-$LaVO_4$) nanocrystals controlled by surface chemistry. Some *t*-$LaVO_4$ nanocrystals with different morphologies were prepared via the hydrothermal method by tuning the pH of the growth solution. The authors perform first-principles calculations to examine the relaxed surface structures and to calculate the surface energies and surface tensions of all surfaces under different passivated conditions. Their results showed

* Corresponding author.
E-mail address: andres@qfa.uji.es (J. Andrés).

http://dx.doi.org/10.1016/j.cplett.2016.08.013
0009-2614/

that the aspect ratio and the exposed facets of the nanocrystals changed as the acidity of the surface conditions changed. This was in good agreement with their experimental findings.

In this communication, we describe the development of a model based on the Wulff construction [32], which can be used to explicitly predict the evolution of morphologies in different environments, as recently developed by our research group [28,29,33]. This model includes a detailed configurational analysis of the different facets and allows us to explain and rationalize the experimental results of Li et al. [24]. By carrying out atomistic simulations elucidating the diverse atomic-scale structures of a set of low-index surfaces (110), (100), (111), (001) and (101) of *t*-$LaVO_4$, we show that it is possible to achieve the same final results without doing many quantum calculations with high computational demand. A correlation was found between the broken bonding density (D_b) and the surface energy. The relaxed structures and surface energies were used to obtain a complete array of accessible morphologies. This method provides an approach with both predictive and explanatory capabilities. The calculated diagrams relate the crystal growth conditions with the observed morphologies in an attempt to rationalize the morphologies obtained under different experimental conditions.

2. Theoretical method and computational procedure

Calculations related to *t*-$LaVO_4$ were performed using DFT and implemented in the Vienna *ab initio* simulation package (VASP) in order to find an ideal structure in *vacuum* [34,35]. The Kohn-Sham equations were solved by means of the Perdew–Burke–Ernzerhof (PBE) exchange-correlation functional [36] and the electron-ion interaction was described by the projector-augmented-wave method [34,37]. The plane-wave expansion was truncated at a cut-off energy of 520 eV. For bulk and surfaces calculations, a $(4 \times 4 \times 4)$ and $(4 \times 4 \times 1)$ Monkhorst-Pack special k-points grid was used, respectively. The positions of all atoms, both in the bulk and on the surfaces, were allowed to relax. The conjugated gradient energy minimization method was used to obtain relaxed systems; this was accomplished by requiring the forces experienced by each atom to be smaller than 0.01 eV $Å^{-1}$. Surface calculations were done by considering slabs with thicknesses of up to ~20 Å. This was done to obtain careful descriptions of the surfaces and to reach convergence on the corresponding energy surface values. A *vacuum* spacing of 15 Å was introduced in the z-direction so that the surfaces would not interact with each other. Surface models containing 6, 4, 4, 6 and 9 molecular units for the (001), (101), (110), (100) and (111) surfaces, respectively, were used in the calculations. These represent all low index surfaces and were modeled using stoichiometric systems. It is worth noting that the (110), and (100) surfaces are O_2-terminated, and the (111) surface is O-terminated, while (001) is LaV and O_2-terminated, and the (101) surface is La-terminated. Fig. 1 depicts the surface representation of the *t*-$LaVO_4$ used in the calculations.

The conventional approach to the quantitative study of surface morphological properties is based on the classical work of Georg

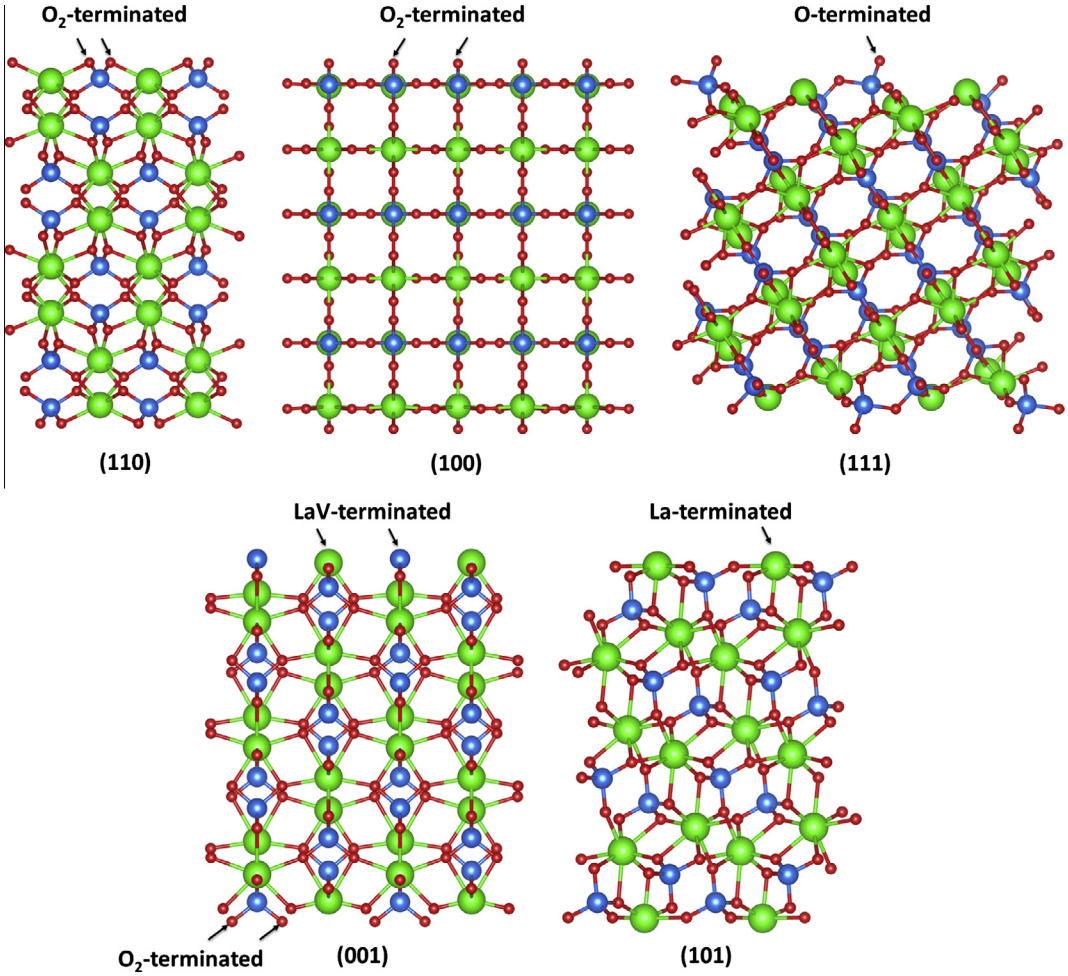

Fig. 1. Surface models of (110), (100), (111), (001) and (101) for *t*-$LaVO_4$. The green, blue and red represent La, V and O atoms, respectively.

Wulff in the beginning of the 20th century [32]. The Wulff construction has been successfully used in materials science to obtain the shapes of materials, including nanomaterials [38–40]. The surface energy (E_{surf}) is defined as the total energy per repeating cell of the slab (E_{slab}) minus the total energy of the perfect crystal per molecular unit (E_{bulk}) multiplied by the number of molecular units of the surface (n), divided by the surface area per repeating cell of the two sides of the slab, as follows:

$$E_{surf} = \frac{E_{slab} - nE_{bulk}}{2A}$$

The broken bonding density (D_b) index proposed by Gao et al. [41] was used. By means of D_b values it is possible to verify the surface stability and analyze the number of broken bonds per area of the surface. In the D_b equation, N_b is the number of broken bonds per unit cell area on a particular surface and A is the surface area of the unit cell.

$$D_b = \frac{N_b}{A}$$

Table 1
Values of E_{suf}, number of broken bonds, area, and broken bonding density (D_b) calculated for t-$LaVO_4$.

Surface	E_{surf} (J m^{-2})	Broken bonds	Area (nm^2)	D_b (nm^{-2})
(100)	0.39	8	0.50	16.0
(110)	0.59	8	0.35	22.9
(101)	0.76	12	0.38	31.6
(111)	1.04	28	0.91	30.8
(001)	2.87	20	0.57	35.1

3. Results and discussion

Table 1 lists the values of the surface energies as well as the broken bonding density (D_b) of the faces used in the Wulff construction. According to the DFT calculations, the order of stability of the surfaces is (100) > (110) > (101) > (111) > (001).

The D_b method has shown certain value due to its simplicity and accuracy in basic systems [29,41]. These results can be directly related to the order and disorder of surface stability; higher D_b values represent the presence of a larger quantity of defects on the surface (broken bonds), indicating an unstable surface. For t-$LaVO_4$, the D_b results indicate the following order (100) > (110) > (111) > (101) > (001). Therefore, these results are the inverse of those found for the (101) and (111) surfaces energy. This can be attributed to the complexity of this structure which involves different kinds of bonds with different energies and this method just take into account the number of broken bonds, independent of the type. In this way, a higher number of broken bonds increase the quantitative accuracy of the method in this structure. Nevertheless, the method showed a fast way to start the surfaces studies.

It is known that morphologies can undergo changes because of differences in the environments in which they are synthesized. These differences may include the presence of surfactants and impurities, and differences in solvents, temperature, and synthetic routes. From the E_{surf} values and the Wulff construction, it is possible to obtain the morphologies of t-$LaVO_4$ in *vacuum*.

By assuming the ideal morphology in *vacuum* as a starting point (see the center of Fig. 2), it was possible to create all of the morphological routing changes caused by surface energy variation that take into account the (110), (100), (111), (001) and (101)

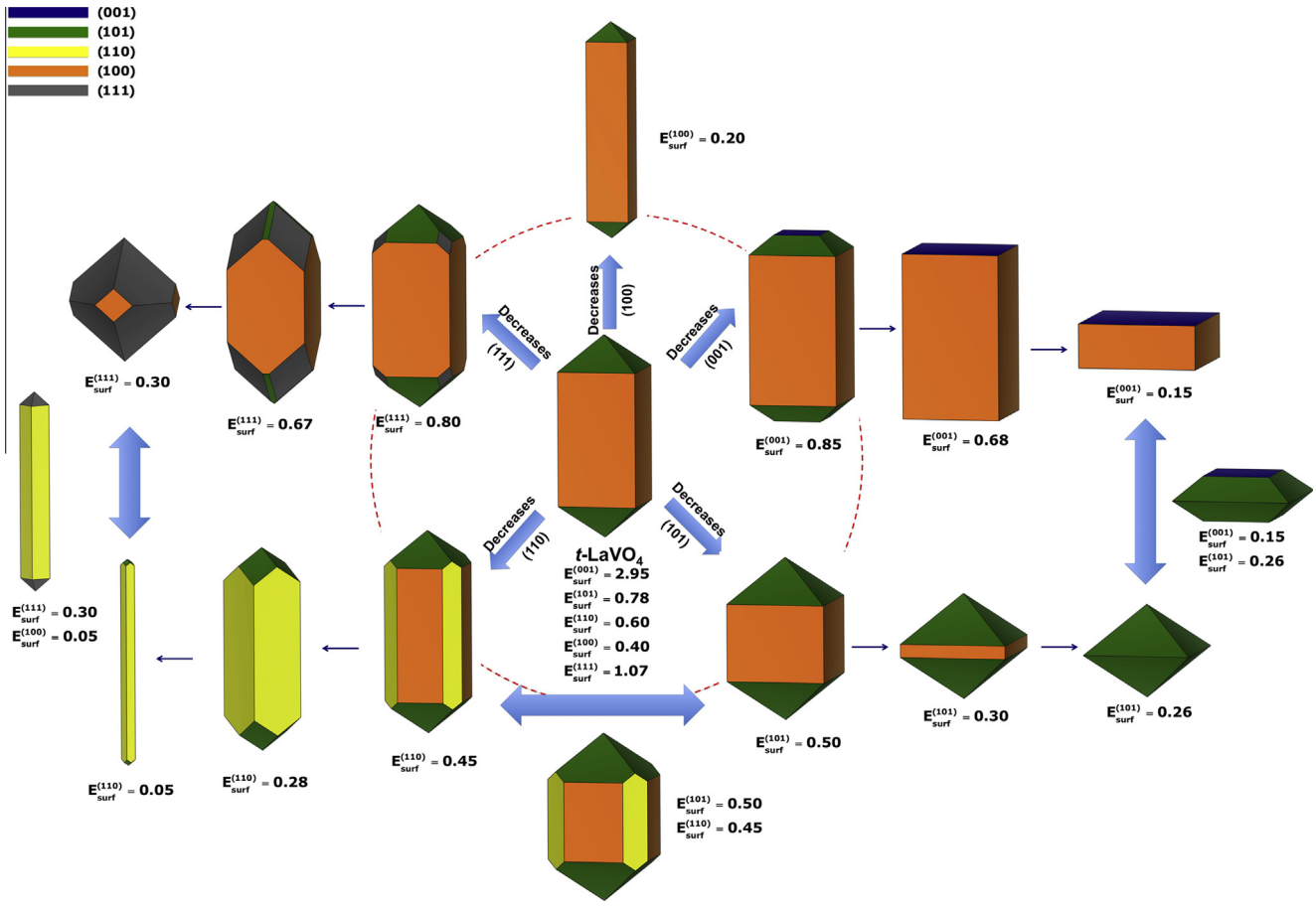

Fig. 2. Ideal morphology (in the center) and map of a few morphologies of t-$LaVO_4$. Surface energy is in J m^{-2}.

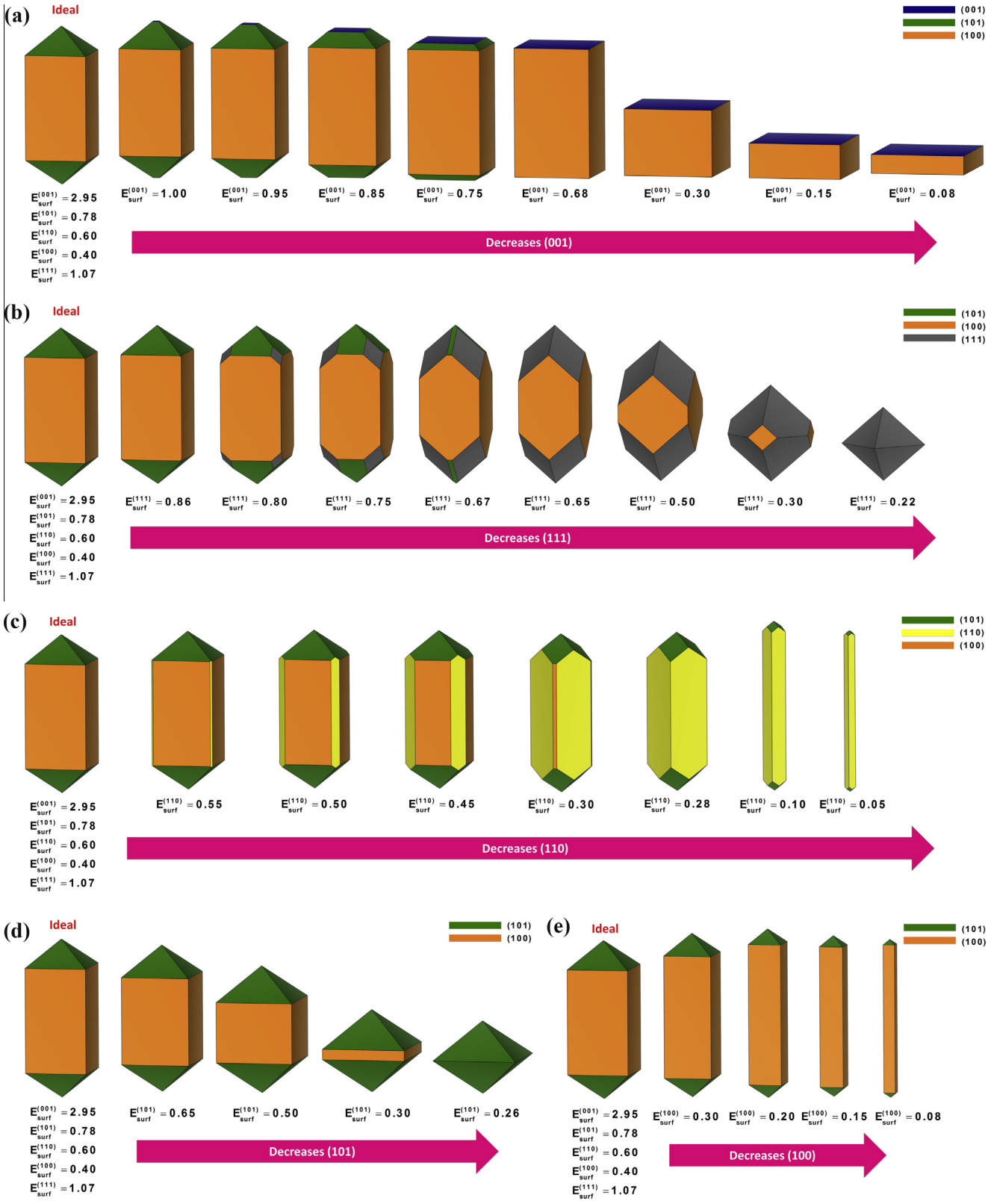

Fig. 3. Morphologies of *t*-$LaVO_4$ when the values of E_{surf} decrease for (a) the (0 0 1) surface; (b) the (1 1 1) surface; (c) the (1 1 0) surface; (d) the (1 0 1) surface and (e) the (1 0 0) surface. Surface energy is in J m^{-2}.

surfaces. This simple strategy is based on the modulation of the relationship between the surface stabilities of the different faces and the areas of those parts which are exposed in the final shape. The map of available morphologies of *t*-$LaVO_4$ is displayed in Fig. 2. Fine-tuning of the desired morphologies can be achieved by controlling the values of the E_{surf} of the different surfaces. This can

be a powerful tool to evaluate the morphologies of materials because of the difficulty in simulating all the details in a reaction system that interacts with each surface [28,29,33].

Fig. 3 depicts a group of morphologies obtained by decreasing the surface energy in small amounts of the (001), (111), (110), (101) and (100).

As was mentioned earlier, the effect of solution acidity on the morphology of as-synthetized *t*-$LaVO_4$ nanocrystals was reported by Li et al. [24]. In their study, the authors prepared nanocrystals using a hydrothermal method in conditions of several different levels of acidity: most-acidic, highly-acidic, moderately acidic and weakly acidic. To compare the resulting morphologies, they simulated these conditions using a 2×1 supercell for all surface passivation. Li et al. [24] demonstrated that the (001) surface is the most affected by the pH shift; its E_{surf} decreased as the fraction of hydrogen in the adsorbates decreased, while the E_{surf} of the (100) and (101) surfaces first increased and then decreased. The difference of the values for the surface energies of (100), (101) and (001) calculated and those obtained by Li et al. [24] may be due to the different functional used in the calculation. Nevertheless the order of stability is the same.

However, here we show that it is possible to achieve the same final results, with the exception of the advantage to predict, without doing many quantum calculations with high computational demand (such as supercell and adsorption of atoms or molecules). Starting with the ideal morphology we decreased the (001) surface energy, as shown in Fig. 3a, and found it possible to observe not only morphologies similar to those synthetized by Li el at. [24], but also more possibilities. To adjust the elongation of the particle, it is necessary to change the (101) energy surface, which is responsible for this part of the structure. When the (101) surface energy decreases, the exposed area of the surface increases and the relative area of (100) decreases causing the structure to become compressed, or less elongated (see Fig. 3d). Therefore, the morphologies of *t*-$LaVO_4$ are controlled by (001), (101) and (100) surface energies.

Material mapping can be used as a guide for experimental researchers in order to evaluate where synthetic modifications interact in a more pronounced way. Some published papers regarding *t*-$LaVO_4$ report various experimental morphologies [42–46]. In these papers, it is possible to find similarities between particles of the same phase when compared to the morphology map. For an accurate comparison, it is necessary to perform a more systematic study of the morphology. This is because the size of the particles makes precise determinations regarding the exposed planes difficult from an experimental perspective. It is worth noting that the simulation does not take into account the formation of particles via any secondary process such as aggregation and coalescence of primarily particles.

4. Conclusions

The study of a material's morphological changes based on theoretical calculation can be used to gain a better understanding of the control of its growth and to provide a more reasonable explanation about its mechanisms of transformation. In this communication, tetragonal phase $LaVO_4$ is investigated by performing theoretical calculations on the mechanism of the morphology transformation. The present strategy provides a perspective for further studying the surface structure and other physical and chemical related applications. The calculated morphology maps must be used as guide for experimentalists to analyze and discuss the results that they obtain by means of Field Emission Gun-Scanning Electron Microscopy (FEG-SEM) and/or Transmission Electron Microscopy (TEM). This methodology clearly show the exposed faces and are capable of explaining the formation of complex morphologies, such as pipes, and hollow spheres. We used this guide with experimental morphologies of different binary oxides such as: Co_3O_4, α-Fe_2O_3, and In_2O_3, as well as metals and metal oxides such as: Ag, anatase TiO_2, $BaZrO_3$, and α-Ag_2WO_4, and $BaWO_4$. However, one must recognize that the results presented here are for ideal systems in *vacuum*. There are important factors involved in a synthesis process that affect the final shape of the end product, including the precursor, solvent, reducing agent, ligand agent, and capping agent. In addition, the presence of defects and impurities may change growth paths and energetics. Both factors can change the morphology of the final product. Further calculations which include these effects will help to improve our understanding of the atomic nature of the observed growth modes and put our understanding of the final morphology on a firmer footing.

Acknowledgments

This work was financially supported by the following Spanish and Brazilian research funding institutions: *PrometeoII*/2014/022 and ACOMP/2014/270 projects (Generalitat-Valenciana), Ministerio de Economia y Competitividad (CTQ2012-36253-C03-02), FAPESP (2013/07296-2 and 2013/26671-9), CNPq (479644/2012-8, 350711/2012-7, 304531/2013-8 and 151136/2013-0). CAPES and Programa de Cooperación Científica con Iberoamerica (Brasil) of Ministerio de Educación (PHBP14-00020). J.A. acknowledges to Ministerio de Economia y Competitividad, 'Salvador Madariaga' program, PRX15/00261. M.M.F. acknowledges CAPES for PNPD scholarship.

References

[1] A.R. Tao, S. Habas, P. Yang, Shape control of colloidal metal nanocrystals, Small 4 (2008) 310–325.
[2] C. Burda, X. Chen, R. Narayanan, M.A. El-Sayed, Chemistry and properties of nanocrystals of different shapes, Chem. Rev. 105 (2005) 1025–1102.
[3] J. Wang, C. Xu, G. Lv, Formation processes of CuCl and regenerated Cu crystals on bronze surfaces in neutral and acidic media, Appl. Surf. Sci. 252 (2006) 6294–6303.
[4] F. Zaera, New challenges in heterogeneous catalysis for the 21st century, Catal. Lett. 142 (2012) 501–516.
[5] Y. Xia, X. Xia, H.-C. Peng, Shape-controlled synthesis of colloidal metal nanocrystals: thermodynamic versus kinetic products, J. Am. Chem. Soc. 137 (2015) 7947–7966.
[6] S.J.L. Billinge, I. Levin, The problem with determining atomic structure at the nanoscale, Science 316 (2007) 561–565.
[7] J. Goniakowski, F. Finocchi, C. Noguera, Polarity of oxide surfaces and nanostructures, Rep. Prog. Phys. 71 (2008) 016501.
[8] C. Noguera, J. Goniakowski, Polarity in oxide nano-objects, Chem. Rev. 113 (2013) 4073–4105.
[9] D.A. Tompsett, S.C. Parker, P.G. Bruce, M.S. Islam, Nanostructuring of β-MnO_2: the important role of surface to bulk ion migration, Chem. Mater. 25 (2013) 536–541.
[10] A. Karim, S. Fosse, K.A. Persson, Surface structure and equilibrium particle shape of the $LiMn_2O_4$ spinel from first-principles calculations, Phys. Rev. B 87 (2013) 075322.
[11] N. Li, H. Dong, H. Dong, J. Li, W. Li, G. Niu, X. Guo, Z. Wu, L. Wang, Multifunctional perovskite capping layers in hybrid solar cells, J. Mater. Chem. A 2 (2014) 14973–14978.
[12] A.S. Barnard, Direct comparison of kinetic and thermodynamic influences on gold nanomorphology, Acc. Chem. Res. 45 (2012) 1688–1697.
[13] A. Seyed-Razavi, I.K. Snook, A.S. Barnard, Origin of nanomorphology: does a complete theory of nanoparticle evolution exist?, J Mater. Chem. 20 (2010) 416–421.
[14] F. Zasada, W. Piskorz, P. Stelmachowski, A. Kotarba, J.-F.O. Paul, T. Płociński, K.J. Kurzydłowski, Z. Sojka, Periodic DFT and HR-STEM studies of surface structure and morphology of cobalt spinel nanocrystals. Retrieving 3D shapes from 2D images, J. Phys. Chem. C 115 (2011) 6423–6432.
[15] D.G. Stroppa, L.A. Montoro, A. Beltrán, T.G. Conti, R.O. da Silva, J. Andrés, E.R. Leite, A.J. Ramirez, Dopant segregation analysis on Sb:SnO_2 nanocrystals, Chem. – Eur. J. 17 (2011) 11515–11519.
[16] A. Beltrán, J. Andrés, E. Longo, E.R. Leite, Thermodynamic argument about SnO_2 nanoribbon growth, Appl. Phys. Lett. 83 (2003) 635–637.

[17] E.R. Leite, T.R. Giraldi, F.M. Pontes, E. Longo, A. Beltrán, J. Andrés, Crystal growth in colloidal tin oxide nanocrystals induced by coalescence at room temperature, Appl. Phys. Lett. 83 (2003) 1566–1568.
[18] D.G. Stroppa, L.A. Montoro, A. Campello, L. Gracia, A. Beltran, J. Andres, E.R. Leite, A.J. Ramirez, Prediction of dopant atom distribution on nanocrystals using thermodynamic arguments, Phys. Chem. Chem. Phys. 16 (2014) 1089–1094.
[19] M.R.D. Bomio, R.L. Tranquilin, F.V. Motta, C.A. Paskocimas, R.M. Nascimento, L. Gracia, J. Andres, E. Longo, Toward understanding the photocatalytic activity of PbMoO4 powders with predominant (111), (100), (011), and (110) facets. A combined experimental and theoretical study, J. Phys. Chem. C 117 (2013) 21382–21395.
[20] V.M. Longo, L. Gracia, D.G. Stroppa, L.S. Cavalcante, M. Orlandi, A.J. Ramirez, E. R. Leite, J. Andrés, A. Beltrán, J.A. Varela, E. Longo, A joint experimental and theoretical study on the nanomorphology of $CaWO_4$ crystals, J. Phys. Chem. C 115 (2011) 20113–20119.
[21] K. Qi, D. Li, J. Fu, L. Zhu, X. Duan, Q. Qin, G. Wang, W. Zheng, Elucidating ionic liquid environments that affect the morphology of TiO_2 nanocrystals: a DFT+D study, J. Phys. Chem. C 118 (2014) 23320–23327.
[22] W. Piskorz, J. Gryboś, F. Zasada, P. Zapała, S. Cristol, J.-F. Paul, Z. Sojka, Periodic DFT study of the tetragonal ZrO_2 nanocrystals: equilibrium morphology modeling and atomistic surface hydration thermodynamics, J. Phys. Chem. C 116 (2012) 19307–19320.
[23] A. Whiteside, C.A.J. Fisher, S.C. Parker, M. Saiful Islam, Particle shapes and surface structures of olivine $NaFePO_4$ in comparison to $LiFePO_4$, Phys. Chem. Chem. Phys. 16 (2014) 21788–21794.
[24] P. Li, X. Zhao, C.-J. Jia, H. Sun, Y. Li, L. Sun, X. Cheng, L. Liu, W. Fan, Mechanism of morphology transformation of tetragonal phase $LaVO_4$ nanocrystals controlled by surface chemistry: experimental and theoretical insights, Cryst. Growth Des. 12 (2012) 5042–5050.
[25] E. Kanaki, S. Gohr, C. Mueller, B. Paulus, Theoretical study on the morphology of MgF2 nanocrystals at finite temperature and pressure, Surf. Sci. 632 (2015) 158–163.
[26] Y. Li, J. Zhang, F. Yang, J. Liang, H. Sun, S. Tang, R. Wang, Morphology and surface properties of $LiVOPO_4$: a first principles study, Phys. Chem. Chem. Phys. 16 (2014) 24604–24609.
[27] V.L. Deringer, R. Dronskowski, From atomistic surface chemistry to nanocrystals of functional chalcogenides, Angew. Chem. Int. Ed. 54 (2015) 15334–15340.
[28] J. Andrés, L. Gracia, A.F. Gouveia, M.M. Ferrer, E. Longo, Effects of surface stability on the morphological transformation of metals and metal oxides as investigated by first-principles calculations, Nanotechnology 26 (2015) 405703–405713.
[29] M.M. Ferrer, A.F. Gouveia, L. Gracia, E. Longo, J. Andres, A 3D platform for the morphology modulation of materials: first principles calculations on the thermodynamic stability and surface structure of metal oxides: Co_3O_4, α-Fe_2O_3, and In_2O_3, Modell. Simul. Mater. Sci. Eng. 24 (2016) 025007–025016.
[30] A. Groß, Theoretical Surface Science: A Microscopic Perspective, Springer, Berlin, 2009.
[31] A.S. Barnard, Modelling of nanoparticles: approaches to morphology and evolution, Rep. Prog. Phys. 73 (2010) 086502.
[32] G. Wulff, On the question of speed of growth and dissolution of crystal surfaces, Z. Kristallogr. 34 (1901) 449–530.
[33] M.C. Oliveira, L. Gracia, I.C. Nogueira, M.F.d. Carmo Gurgel, J.M.R. Mercury, E. Longo, J. Andrés, Synthesis and morphological transformation of $BaWO_4$ crystals: experimental and theoretical insights, Ceram. Int. 42 (2016) 10913–10921.
[34] G. Kresse, J. Furthmuller, Efficiency of ab-initio total energy calculations for metals and semiconductors using a plane-wave basis set, Comput. Mater. Sci. 6 (1996) 15–50.
[35] G. Kresse, J. Hafner, Ab-initio molecular-dynamics simulation of the liquid-metal amorphous-semiconductor transition in germanium, Phys. Rev. B: Condens. Matter Mater. Phys. 49 (1994) 14251–14269.
[36] J.P. Perdew, K. Burke, M. Ernzerhof, Generalized gradient approximation made simple, Phys. Rev. Lett. 77 (1996) 3865–3868.
[37] G. Kresse, D. Joubert, From ultrasoft pseudopotentials to the projector augmented-wave method, Phys. Rev. B: Condens. Matter Mater. Phys. 59 (1999) 1758–1775.
[38] A. Gurlo, Nanosensors: towards morphological control of gas sensing activity. SnO_2, In_2O_3, ZnO and WO_3 case studies, Nanoscale 3 (2011) 154–165.
[39] G.D. Barmparis, Z. Lodziana, N. Lopez, I.N. Remediakis, Nanoparticle shapes by using Wulff constructions and first-principles calculations, Beilstein J. Nanotechnol. 6 (2015) 361–368.
[40] A. Hellman, K. Honkala, I.N. Remediakis, A. Logadottir, A. Carlsson, S. Dahl, C.H. Christensen, J.K. Norskov, Ammonia synthesis and decomposition on a Ru-based catalyst modeled by first-principles, Surf. Sci. 603 (2009) 1731–1739.
[41] Z.-Y. Gao, W. Sun, Y.-H. Hu, Mineral cleavage nature and surface energy: anisotropic surface broken bonds consideration, T. Nonferr. Metal. Soc. 24 (2014) 2930–2937.
[42] J. Ma, Q. Wu, Y. Ding, Selective synthesis of monoclinic and tetragonal phase LaVO(4) nanorods via oxides-hydrothermal route, J. Nanopart. Res. 10 (2008) 775–786.
[43] J. Zhang, J. Shi, J. Tan, X. Wang, M. Gong, Morphology-controllable synthesis of tetragonal $LaVO_4$ nanostructures, CrystEngComm 12 (2010) 1079–1085.
[44] Z. Xu, C. Li, Z. Hou, C. Peng, J. Lin, Morphological control and luminescence properties of lanthanide orthovanadate LnVO(4) (Ln = La to Lu) nano-/microcrystals via hydrothermal process, CrystEngComm 13 (2011) 474–482.
[45] L.-P. Wang, L.-M. Chen, Controllable synthesis and luminescent properties of $LaVO_4$: Eu nanocrystals, Mater. Charact. 69 (2012) 108–114.
[46] B. Xie, G. Lu, Y. Wang, Y. Guo, Y. Guo, Selective synthesis of tetragonal $LaVO_4$ with different vanadium sources and its luminescence performance, J. Alloys Compd. 544 (2012) 173–180.